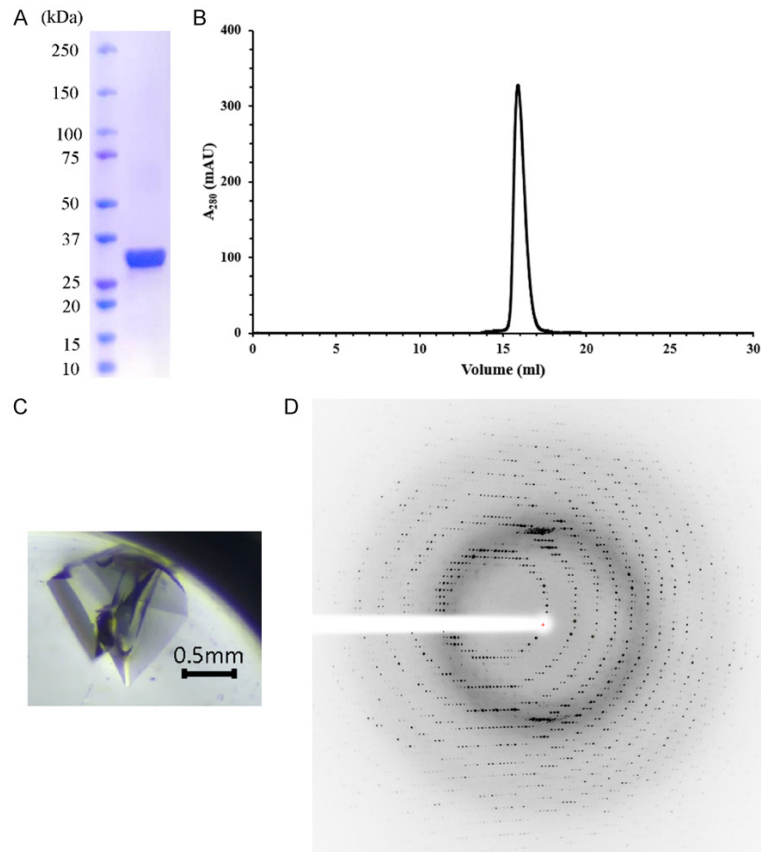


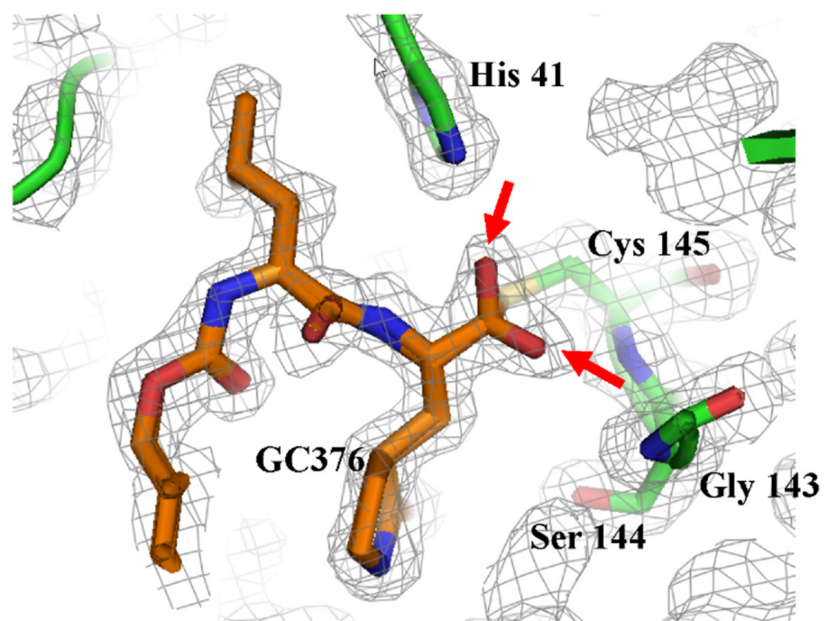
## SARS-CoV-2 M<sup>pro</sup> inhibition by GC376



**Figure S1.** Purification, crystallization, and data collection of SARS-CoV-2 M<sup>pro</sup> with GC376. A. The SDS-PAGE of purified SARS-CoV-2 M<sup>pro</sup>. The estimated molecular weight is consistent with its theoretical molecular weight of 33.8 kDa. B. Size-exclusion chromatography of SARS-CoV-2 M<sup>pro</sup>. C. Crystal of SARS-CoV-2 M<sup>pro</sup> in complex with GC376 grown in 0.1 M Bis-Tris propane pH 6.5, 0.02 M sodium/potassium phosphate, 20% (w/v) PEG3350, using sitting-drop vapor-diffusion method. D. Diffraction pattern of the crystal of SARS-CoV-2 M<sup>pro</sup> with GC376 collected using a Rayonix MX300HE CCD detector on beamline 15A1 at NSRRC, Taiwan.

SARS-CoV-2 M<sup>pro</sup> inhibition by GC376

A



B

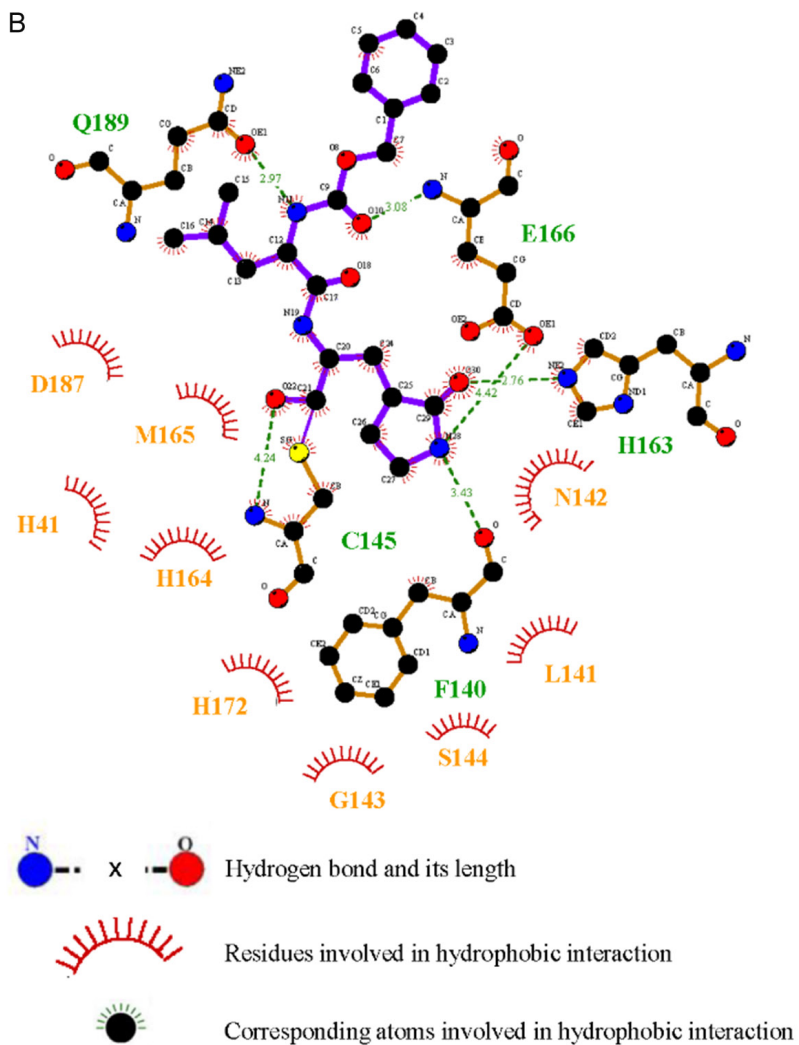


**Figure S2.** Detailed distribution of hydrophilic and hydrophobic interactions at the substrate-binding site of SARS-CoV-2 M<sup>pro</sup> in complex with GC376. A. Electronic map of GC376 in the binding pocket of SARS-CoV-2 M<sup>pro</sup>. GC376 covalently linked to Cys145. Two different orientation of hemithioacetal group observed in electron-density map are indicated by arrows. B. Ligplot representation of the hydrogen bonding and hydrophobic interactions at the catalytic center of SARS-CoV-2 M<sup>pro</sup> in complex with GC376.